

Composite Preambles Based on Differential Phase Rotations for Grant-free Random Access Systems

Yang Wang, *Student Member, IEEE*, Wenjun Xu, *Senior Member, IEEE*, Markku Juntti, *Fellow, IEEE*,
Jiaru Lin, *Member, IEEE*, Miao Pan, *Senior Member, IEEE*

Abstract—With the advantages of low signaling overhead and latency, grant-free random access (GFRA) becomes a promising technology for supporting massive machine-type communications (mMTC), but poses new challenges for active user detection (AUD) and channel estimation (CE), whose performance mainly depends on the preamble detection. In this paper, we design the composite preamble based on differential phase rotations by aggregating orthogonal Zadoff-Chu (ZC) sequences and multiple root ZC sequences with differential phase rotations to reduce the probability of preamble collisions, thereby improving the performance of AUD and CE. In particular, differential phase rotations extend the preamble set size so that users colliding in orthogonal sequences can be distinguished by phase rotations. In addition, it also reduces non-orthogonal interference and thus reduces CE errors. The preamble detection algorithm and CE scheme are proposed, along with the theoretical analysis of AUD and CE performance to verify the effectiveness of the designed preamble. In addition, the proposed preamble is extended to combine phase rotations with cyclic shifts to further enlarge the preamble set size with low non-orthogonality. Simulation results show that the proposed composite preamble outperforms existing preambles in terms of the probability of detection and CE accuracy.

Index Terms—Composite preambles, massive machine-type communications, preamble collision, user detection.

I. INTRODUCTION

THE past few decades have witnessed the proliferation of Internet-of-Things (IoT) systems, especially the recent rapid rise of machine-type communications (MTC) devices that access the Internet through wireless networks, such as vehicles, sensors, household appliances and smart medical devices [1]. Statistics show that MTC devices are expected to

This work was supported in part by the National Natural Science Foundation of China, under grant 62293485, in part by the Fundamental Research Funds for the Central Universities, under grant 2022RC18, in part by the Academy of Finland ROHM project (grant 319485) and 6G Flagship (grant 346208), in part by the BUPT Excellent Ph.D. Students Foundation (CX2021207), and in part by the China Scholarship Council.

Y. Wang and W. Xu are with the State Key Laboratory of Network and Switching Technology, Beijing University of Posts and Telecommunications, Beijing 100876, China; W. Xu is also affiliated with the Department of Mathematics and Theories, Peng Cheng Laboratory, Shenzhen 518066, China (e-mail: (wy, wjxu@bupt.edu.cn).

J. Lin is with the Key Lab of Universal Wireless Communications, Ministry of Education, Beijing University of Posts and Telecommunications, Beijing, P. R. China (e-mail: jrlin@bupt.edu.cn).

M. Juntti is with the Centre for Wireless Communications-Radio Technologies, University of Oulu, 90014 Oulu, Finland (e-mail: markku.juntti@oulu.fi).

M. Pan is with the Department of Electrical and Computer Engineering, University of Houston, Houston, TX 77004 USA (e-mail: miaopan.ufl@gmail.com).

Corresponding author: Wenjun Xu (wjxu@bupt.edu.cn).

account for more than 50% of devices connected to communication networks by 2023 [2], [3]. In line with this trend, ITU has identified massive machine-type communications (mMTC) as one of the three representative scenarios for 5G wireless systems [4].

Typically, mMTC is characterized by massive connections, sporadic transmission, and short data packets. In such cases, the existing grant-based random access (RA) protocol is not desirable due to the excessive latency and signaling overhead. Therefore, the grant-free RA (GFRA) protocol is proposed to accommodate mMTC, which allows devices to transmit packets consisting of preamble and data at any time without getting a grant from the base station (BS), and thus reducing the signaling overhead and latency [5]. Moreover, to support massive connectivity, grant-free access is generally used in non-orthogonal multiple access (NOMA) and multiple-input and multiple-output (MIMO) networks [5]–[7].

In GFRA systems, since the BS has no information about user scheduling, the active user detection (AUD) and channel estimation (CE) should be performed first by processing preambles to facilitate the subsequent data detection. The existing schemes mostly assume that the user accesses the channel with a unique preamble, and then detect the presence of preambles to distinguish between active and inactive devices [8]–[11]. However, it is difficult to guarantee the uniqueness of preambles. On the one hand, as the choice of preambles is random and independent, it is highly likely that two users choose the same preamble, i.e., a preamble collision occurs. On the other hand, the number of available preambles (i.e., preamble set size) is limited due to the limited preamble length, and the probability of preamble collisions will be increased with the growth of the number of MTC devices. In the case of collisions, the accuracy of the AUD is degraded, resulting in a significant increase in the CE and data detection errors. Therefore, preamble collisions are the bottleneck of performance.

Several orthogonal sequence-based schemes have been proposed to resolve the problem. It has been demonstrated that when the number of antennas is sufficiently large, orthogonal preambles enable accurate AUD and CE, and the performance of GFRA systems depends mainly on the preamble length [12]. To detect users suffering from preamble collisions, a non-orthogonal random access (NORA) scheme has been proposed, which distinguishes collided users based on the difference in times of arrival (ToA) [13]. However, the collided users cannot be detected when their ToA are close to each other. Then, more attention is paid to assembling orthogonal preambles in

non-orthogonal manners to enlarge the preamble pool and thus avoiding preamble collisions.

Protocols that send preambles with different patterns have been proposed, including sending preambles by hopping over multiple slots [14] and inserting preambles in designated slots [15]. These patterns mitigate collisions, but also pose challenges for AUD and CE. Inspired by [14] and [15], a super preamble (S-preamble) that sends multiple orthogonal preambles in succession has been proposed in [16], which enlarges the preamble set size at the cost of excessively long preamble transmission phases. Subsequently, an improved S-preamble has been proposed in [17] to expand the preamble pool without increasing the preamble length, which divides a transmission phase into several consecutive subphases and sends a shorter orthogonal preamble in each sub-phase. Nevertheless, it cannot be ignored that the performance of CE degrades due to the non-orthogonality of S-preambles, and it is shown that preambles with subphases not always outperform those without them [18]. Therefore, preambles without subphases have been proposed. Specifically, non-orthogonal preambles formed by the union of two orthogonal preamble sets have been proposed in [19] and [20], where the selection of preamble sets obeys predefined rules. Preambles consisting of fixed preambles and random sequences have been proposed in [21], where the random sequences have been used for data scrambling. Note that the preambles in [21] are carefully designed for two pre-defined categories of users, and there are one-to-one mapping relationships between fixed preambles and random sequences. The predefined rules and one-to-one mappings reduce the non-orthogonal interference, but also limit the preamble set size to some extent. Besides, preambles formed by the sum of randomly selected orthogonal sequences have also been proposed, where sequences are transmitted at different power levels [22], [23]. The power levels expand the preamble pool but reduce the accuracy of the AUD.

In addition to assembling orthogonal sequences, a more straightforward approach is to use non-orthogonal sequences as preambles, which naturally increases the preamble set size despite decreasing the accuracy of the detection. In detail, preambles based on Bernoulli sequences [24], m-sequences [25], Gaussian sequences [7] and multiple root Zadoff-Chu (ZC) sequences [6] have been designed, among which Gaussian sequences and multiple root ZC sequences are most widely adopted. The performance of the two sequences is compared in [26], and it is shown that multiple root ZC sequences outperform Gaussian sequences in most cases.

Based on the existing schemes, it can be concluded that preambles based on either orthogonal or non-orthogonal sequences are not competent since orthogonal sequences are not sufficient to support massive connections and non-orthogonal sequences have been criticized for having large interference. Therefore, the key problem becomes how to expand the size of the preamble pool at the cost of lower non-orthogonal interference. Different from existing schemes, we propose the composite preamble by aggregating orthogonal and differential phase rotation-based nonorthogonal sequences to solve the problem. Specifically, the proposed preamble is designed as an orthogonal sequence followed by a non-orthogonal sequence,

where the orthogonal sequences are used to guarantee the performance of AUD and CE of users without orthogonal preamble collisions as well as to reduce the CE errors of collided users. As for the non-orthogonal sequences, they are generated by multiple root ZC sequences with differential phase rotations and users with the same orthogonal preamble collisions can be distinguished by the phase rotations. Note that the utilization of differential phase rotations not only expands the preamble pool, but also reduces the cross-correlation of multiple root ZC sequences, thus, reducing the probability of collisions and improving the performance of CE. At the BS, users without orthogonal preamble collisions can be identified by detecting the orthogonal sequences, and their channel vectors can be estimated accordingly. As for collided users, they are distinguished by processing non-orthogonal sequences to detect the phase rotations, and the channel vectors are estimated with low errors correspondingly.

In this paper, the scheme for constructing composite preambles by adding differential phase rotations to multiple root ZC sequences with the single cyclic shift is given first to illustrate the superiority of phase rotations, including the preamble structure, AUD and CE scheme, the theoretical performance of AUD and CE. Subsequently, the proposed scheme is extended to multiple root ZC sequences with randomly selected cyclic shifts, and the combination of phase rotations and cyclic shifts is given theoretically to further expand the preamble set size using cyclic shifts without increasing the non-orthogonal interference.

The novelty and contribution of this paper are summarized as follows.

- 1) The differential phase rotation-based composite preamble considering multiple root ZC sequences with the single cyclic shift is proposed, which reduces the non-orthogonal interference while enlarging the preamble set size by utilizing differential phase rotations.
- 2) Based on the proposed preamble, the detection algorithm and CE scheme are proposed, and the theoretical analysis of AUD and CE is derived to verify the superiority of differential phase rotations.
- 3) The extension to multiple root ZC sequences with randomly selected cyclic shifts is given, and the theoretical analysis of phase rotations-cyclic shifts combination is presented to further expand the preamble set size.

The rest of this paper is organized as follows. In Section II, the system model of GFRA system is illustrated. In Section III, the designed preambles and detection algorithm are proposed, and the performance analysis is also given. Section IV extends the proposed preamble to multiple root ZC sequences with randomly selected cyclic shifts. Simulation results are presented in section V. We conclude the paper in Section VI.

Notation: The matrices and vectors are denoted by boldface upper and lower case letters, respectively. \mathbf{I}_M is the $M \times M$ unit matrix. $(\cdot)^T$ and $(\cdot)^H$ are the transpose and complex conjugate transpose operators. $\|\cdot\|$ denotes the Euclidean norm.

II. SYSTEM MODEL

Consider a single-cell grant-free access system as illustrated in Fig. 1, consisting of a BS equipped with M antennas and multiple users. Each user is equipped with a single antenna, and it is assumed that there are K active users uniformly distributed in the cell.

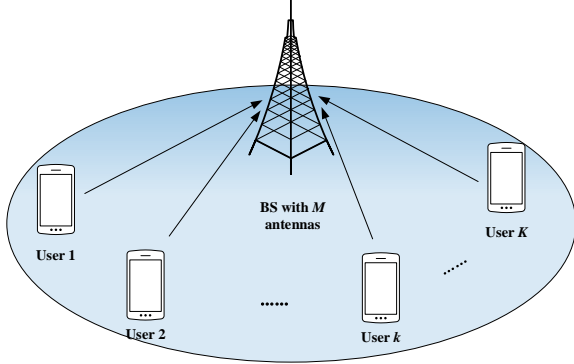


Fig. 1. GFRA system model.



Fig. 2. GFRA transmission model.

As shown in Fig. 2, the user transmits preambles followed by the data to the BS, where the preambles are used for AUD and CE. The preambles are randomly selected from the preamble pool $\mathbf{S} = [\mathbf{s}_1^T, \dots, \mathbf{s}_{l_k}^T, \dots, \mathbf{s}_L^T]^{N \times L}$ with $l_k = 1, \dots, L$. Specifically, \mathbf{s}_{l_k} with index l_k is the preamble selected by user k . N is the length of preamble sequences and L is the size of the preamble pool. If sequences \mathbf{s}_{l_k} ($l_k = 1, \dots, L$) are orthogonal, $L = N$, otherwise, $L > N$. Generally, orthogonal preambles facilitate accurate user detection, but are prone to preamble collisions due to the limited size of the preamble pool. In contrast, non-orthogonal sequences can enlarge the preamble pool at the cost of decreased detection performance.

Denote $\tilde{\mathbf{h}}_k \in \mathbb{C}^{M \times 1}$ as the channel gain between user k and the BS, where $\tilde{\mathbf{h}}_k = \sqrt{h_{dk}} \mathbf{h}_k$ with $\sqrt{h_{dk}}$ is the large-scale fading coefficient related to the distance and $\mathbf{h}_k \sim \mathcal{CN}(0, \mathbf{I}_{M \times 1})$ is the small-scale fading coefficient. Note that the assumption of uncorrelated fading has been widely used in GFRA systems for analysis and simulations [12], [14], [16]–[18]. In addition, it is assumed that the power control is perfect, which means that the received power $P = P_k h_{dk}$ is identical for all active users even though their transmission power P_k is different. Then, the received signal is

$$\mathbf{Y} = \sum_{k=1}^K \sqrt{P} \tilde{\mathbf{h}}_k \mathbf{s}_{l_k} + \mathbf{W} \in \mathbb{C}^{M \times N}, \quad (1)$$

where \mathbf{W} is the the circularly symmetric complex Gaussian (CSCG) noise with zero-mean and variance σ^2 . The signal-to-noise ratio (SNR) is $\gamma = \frac{P}{\sigma^2}$.

Based on the received signal \mathbf{Y} , the BS performs AUD by detecting preambles selected by active users and also estimates channel coefficients to provide information for data detection.

III. PROPOSED PREAMBLE DESIGN

In this section, the composite preamble that assembles the advantages of orthogonal and non-orthogonal sequences is proposed to reduce the probability of preamble collision and thereby improve the performance of AUD and CE. The designed preambles are first given, followed by the detection scheme and performance analysis.

A. Designed preamble

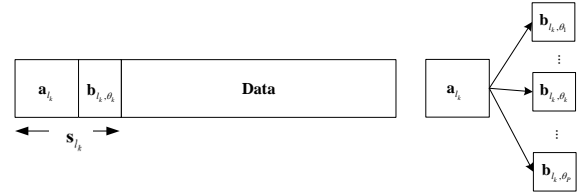


Fig. 3. Designed composite preamble structure.

The designed preamble is shown in Fig. 3, where \mathbf{s}_{l_k} consists of the orthogonal sequence \mathbf{a}_{l_k} and non-orthogonal sequence $\mathbf{b}_{l_k, \theta_k}$. In detail, \mathbf{a}_{l_k} is generated by the single-root ZC sequence, i.e.,

$$a_{l_k}(n) = \exp(-j\pi(n + l_k)(n + l_k + 1)/N_1), \quad (2)$$

with $n = 1, \dots, N_1$. N_1 is the length of \mathbf{a}_{l_k} and $N_1 \geq N/2$. $l_k \in [0, N_1 - 1]$ is the cyclic shift. The single-root ZC sequence has the favorable property that $\|\mathbf{a}_{l_k} \mathbf{a}_{l_k}^H\|^2 = N_1$, but for $l'_k \neq l_k$, $\|\mathbf{a}_{l_k} \mathbf{a}_{l'_k}^H\|^2 = 0$.

As for the non-orthogonal sequence $\mathbf{b}_{l_k, \theta_k}$, it is generated by phase-rotating multiple root ZC sequences, which is expressed as

$$b_{l_k, \theta_k}(n) = \exp\left(\frac{-j\pi l_k(n + c_{l_k})(n + c_{l_k} + 1)}{N_2} - jn\theta_k\right), \quad (3)$$

with $n = 1, \dots, N_2$, $N_2 = N - N_1$. To analyze the performance of phase rotations, it is first assumed that there is a one-to-one mapping relationship between l_k and c_{l_k} . Parameter θ_k is the phase rotation, which is randomly selected from $\Theta = [\theta_1, \theta_2, \dots, \theta_Q]$. Note that there is a relationship between $\mathbf{b}_{l_k, \theta_k}$ and \mathbf{a}_{l_k} , i.e., the cyclic shift of \mathbf{a}_{l_k} is designated as the root of $\mathbf{b}_{l_k, \theta_k}$. Therefore, users selecting the same orthogonal preamble can be distinguished by the non-orthogonal preambles with different phase rotations. Phase rotation enlarges the size of the preamble pool from N to QN_1 , which reduces the probability of preamble collisions. Besides, it helps to reduce the cross-correlation of ZC sequences with different roots, which will be analyzed in detail in Section III-B.

With the composite preambles, the signal received by the BS is expressed as

$$\mathbf{Y} = [\mathbf{Y}_1, \mathbf{Y}_2], \quad (4)$$

where

$$\mathbf{Y}_1 = \sum_{k=1}^K \sqrt{P} \mathbf{h}_k \mathbf{a}_{l_k} + \mathbf{W} \in \mathbb{C}^{M \times N_1}, \quad (5)$$

and

$$\mathbf{Y}_2 = \sum_{k=1}^K \sqrt{P} \mathbf{h}_k \mathbf{b}_{l_k, \theta_k} + \mathbf{W} \in \mathbb{C}^{M \times N_2}. \quad (6)$$

B. Preamble detection

After receiving the signal \mathbf{Y} from the uplink transmission, the BS detects the preambles to identify the active users. First, BS processes \mathbf{Y}_1 to detect which orthogonal sequences have been selected and initially determines whether they have been transmitted by multiple users. If the preamble has been selected by one user, the corresponding active user has been identified. Otherwise, it indicates that the preamble collision has occurred. These collided users are identified by detecting \mathbf{Y}_2 . The detailed detection scheme is as follows.

1) *Orthogonal sequence detection*: In view of the advantageous autocorrelation and cross-correlation properties of the single-root ZC sequence, \mathbf{a}_{l_k} can be detected by calculating the correlation of \mathbf{Y}_1 and $\mathbf{a}_{l_k}^H$, which is

$$\mathbf{g}_1 = \mathbf{Y}_1 \mathbf{a}_{l_k}^H = \sum_{k=1}^K \sqrt{P} \mathbf{h}_k \mathbf{a}_{l_k} \mathbf{a}_{l_k}^H + \mathbf{W} \mathbf{a}_{l_k}^H, \quad (7)$$

If \mathbf{a}_{l_k} has been selected,

$$\mathbf{g}_1 = \sum_{k \in \mathcal{L}_k} \sqrt{P} \mathbf{h}_k \|\mathbf{a}_{l_k}\|^2 + \mathbf{W} \mathbf{a}_{l_k}^H, \quad (8)$$

where \mathcal{L}_k is the set of users which have selected \mathbf{a}_{l_k} as the orthogonal preamble. Otherwise,

$$\mathbf{g}_1 = \mathbf{W} \mathbf{a}_{l_k}^H. \quad (9)$$

The test statistic T_1 is defined as

$$T_1 = \frac{1}{N_1} \|\mathbf{g}_1\|^2. \quad (10)$$

Denote the cases that \mathbf{a}_{l_k} has not been selected and has been selected by only one user as \mathcal{H}_0 and \mathcal{H}_1 , respectively. In the case of \mathcal{H}_0 , T_1 is a random variable that obeys a Chi-square distribution. According to the central limit theorem (CLT), T_1 can be approximated as a Gaussian distribution when N_1 is large [27]–[30], that is

$$T_1 \sim \mathcal{N}(M\sigma^2, M\sigma^2). \quad (11)$$

Similarly, under hypothesis \mathcal{H}_1 , T_1 is approximated by the following Gaussian distribution.

$$T_1 \sim \mathcal{N}(MN_1P + M\sigma^2, 2MN_1P + M\sigma^2). \quad (12)$$

Hence, by comparing T_1 with a threshold, the presence of \mathbf{a}_{l_k} can be detected. The decision rule is given as

$$\begin{cases} \mathcal{H}_0, & T_1 < \lambda_1 \\ \mathcal{H}_1, & T_1 \geq \lambda_1 \end{cases} \quad (13)$$

The threshold λ_1 satisfies that

$$f_{T_1|\mathcal{H}_0}(\lambda_1) = f_{T_1|\mathcal{H}_1}(\lambda_1). \quad (14)$$

where $f_{T_1|\mathcal{H}_0}(\lambda_1)$ and $f_{T_1|\mathcal{H}_1}(\lambda_1)$ are the probability density function of T_1 in the case of \mathcal{H}_0 and \mathcal{H}_1 , which are given as (11) and (37), respectively.

The probability of orthogonal sequence detection is derived as

$$\begin{aligned} P_{d_1} &= Pr(T_1 \geq \lambda_1 | \mathcal{H}_1) \\ &= Q\left(\frac{\lambda_1 - MN_1P - M\sigma^2}{\sqrt{2MN_1P + M\sigma^2}}\right). \end{aligned} \quad (15)$$

If it is detected that \mathbf{a}_{l_k} has been selected, then the next step is to determine if there exists the preamble collision. Denote the size of \mathcal{L}_k as K_c , which is calculated as

$$K_c = \max\left(1, \frac{T_1}{MN_1P}\right). \quad (16)$$

If $K_c = 1$, \mathbf{a}_{l_k} has been selected by only one user and the channel vector is estimated as

$$\hat{\mathbf{h}}_k = \frac{1}{N_1 \sqrt{P}} \mathbf{Y}_1 \mathbf{a}_{l_k}^H. \quad (17)$$

Otherwise, it is stated that there is a preamble collision.

Note that the only concern here is whether K_c is greater than 1, not the exact value of K_c . This is because there may be false alarms, i.e., K_c is larger than the number of actually collided users. The false alarms ensure that the collided users will not be missed and they can be corrected in the non-orthogonal sequence detection.

2) *Interference cancellation*: Since users without preamble collisions have been detected and their channel vectors are estimated, the corresponding non-orthogonal preambles can be removed from \mathbf{Y}_2 to cancel the interference caused by the non-collided users. The residual signal of \mathbf{Y}_2 becomes

$$\mathbf{Y}_{2r} = \mathbf{Y}_2 - \sum_{l_k \in \mathcal{K}_o} \sqrt{P} \hat{\mathbf{h}}_k \mathbf{b}_{l_k, \hat{\theta}_k}, \quad (18)$$

where \mathcal{K}_o is the index set of preambles chosen by non-collided users, and $\hat{\theta}_k$ is the estimated phase rotation selected by user k . To estimate the phase rotation, the correlation between \mathbf{Y}_2 and $\mathbf{b}_{l_k, \theta}$ is considered, i.e.,

$$\mathbf{Y}_2 \mathbf{b}_{l_k, \theta}^H = \sqrt{P} \mathbf{h}_k \mathbf{b}_{l_k, \theta} \mathbf{b}_{l_k, \theta}^H + \nu, \quad (19)$$

where ν is the interference caused by users who choose other orthogonal preambles and noise, and ν is much smaller than $|\sqrt{P} \mathbf{h}_k \mathbf{b}_{l_k, \theta} \mathbf{b}_{l_k, \theta}^H|$ due to the property of multiple root ZC sequences. Therefore, $\mathbf{Y}_2 \mathbf{b}_{l_k, \theta}^H$ mainly depends on

$$\mathbf{b}_{l_k, \theta_k} \mathbf{b}_{l_k, \theta}^H = \sum_{n=1}^{N_2} e^{jn(\theta - \theta_k)}. \quad (20)$$

For the ease of representation, denote $\Delta_\theta = \theta - \theta_k$. If and only if $\Delta_\theta = 0$, $\sum_{n=1}^{N_2} e^{jn(\theta - \theta_k)} = N_2$, otherwise, it is negligible. For example, when $\Delta_\theta = 0.5\pi$,

$$\sum_{n=1}^{N_2} e^{jn(\theta - \theta_k)} = \begin{cases} 0 & N_2 \bmod 4 = 0 \\ j & N_2 \bmod 4 = 1 \\ j-1 & N_2 \bmod 4 = 2 \\ -1 & N_2 \bmod 4 = 3 \end{cases}, \quad (21)$$

where ‘mod’ is the modulo operation. Similar conclusions can be drawn when Δ_θ is equal to other values. Therefore, the estimate of θ_k is obtained as

$$\hat{\theta}_k = \operatorname{argmax}_{\theta \in \Theta} \|\mathbf{Y}_2 \mathbf{b}_{l_k, \theta}^H\|^2. \quad (22)$$

3) *Non-orthogonal sequence detection:* After canceling the interference of the non-collided users, the BS detects non-orthogonal preambles to identify the collided users based on \mathbf{Y}_{2_r} . The set of collided preambles is represented as \mathcal{K}_n , then \mathbf{Y}_{2_r} can be rewritten as

$$\mathbf{Y}_{2_r} = \sum_{l_k \in \mathcal{K}_n} \sqrt{P} \mathbf{h}_k \mathbf{b}_{l_k, \theta_k} + \mathbf{W}. \quad (23)$$

As a result, the correlation of \mathbf{Y}_2 with $\mathbf{b}_{l_k, \theta_q}$ is

$$\mathbf{g}_2 = \mathbf{Y}_{2_r} \mathbf{b}_{l_k, \theta_q}^H = \sqrt{P} \mathbf{h}_k \|\mathbf{b}_{l_k, \theta_q}\|^2 + \nu_{\theta_q} + \nu_{l_k} + \mathbf{W} \mathbf{b}_{l_k, \theta_q}^H, \quad (24)$$

where ν_{θ_q} is the interference caused by users that choose the same l_k but with different phase rotations, which can be expressed as

$$\nu_{\theta_q} = \sum_{\theta'_q \neq \theta_q} \sqrt{P} \mathbf{h}_k \mathbf{b}_{l_k, \theta'_q} \mathbf{b}_{l_k, \theta_q}^H. \quad (25)$$

ν_{l_k} is the interference caused by the collided users choosing other orthogonal preambles, that is,

$$\nu_{l_k} = \sum_{l'_k \in \mathcal{K}_n} \sqrt{P} \mathbf{h}_k \mathbf{b}_{l'_k, \theta} \mathbf{b}_{l_k, \theta_q}^H, \quad l'_k \neq l_k, \theta \in \Theta. \quad (26)$$

As mentioned above, $|\nu_{\theta_q}|$ is negligible. While for $|\nu_{l_k}|$, it is closely related to Δ_θ , $\Delta_c = c'_{l_k} - c_{l_k}$ and $\Delta_k = l'_k - l_k$, which is much less than N_2 . For example, when $N_2 = 32$, given $b_{1,0}(n) = \exp(-j\pi n(n+1)/N_2)$, the cross-correlations of $\mathbf{b}_{1,0}$ and sequences with various l'_k , c'_{l_k} and θ are shown in Table I. In detail, $\theta = 0$ indicates the case where there is no phase rotation and it is used as a benchmark. Values in red represent the case in which the cross-correlation is larger than the benchmark. It is shown that phase rotations reduce the cross-correlation in most cases. In particular, when $l'_k = 4$, $c'_{l_k} = 1$ and $l'_k = 2$, $c'_{l_k} = 2$, the cross-correlation is reduced by almost half. Even though at $l'_k = 2$, $c'_{l_k} = 1$ and $l'_k = 4$, $c'_{l_k} = 2$, $|\nu_{l_k}|$ at some phase rotations are larger than benchmarks, the average cross-correlation $|\bar{\nu}_{l_k}|$ is close to or even less than the benchmark. Note that the conclusion also holds for situations with other values of N_2 , Δ_θ , Δ_c and Δ_k . Therefore, the correlation of non-orthogonal sequences can be decreased by phase-rotating the ZC sequences and thereby reducing the interference and improving the detection performance. Moreover, the preamble set size is enlarged by using phase rotations, which reduces the probability of preamble collision.

In the non-orthogonal sequence detection process, the test statistics is given as

$$T_2 = \frac{1}{N_2} \|\mathbf{g}_2\|^2. \quad (27)$$

TABLE I
 $|\nu_{l_k}|$ VARIES WITH Δ_θ , Δ_c AND Δ_k .

(a) $c'_{l_k} = 1$									
l'_k	$\theta=0$	$\theta=\frac{\pi}{4}$	$\theta=\frac{\pi}{2}$	$\theta=\frac{3\pi}{4}$	$\theta=\pi$	$\theta=\frac{5\pi}{4}$	$\theta=\frac{3\pi}{2}$	$\theta=\frac{7\pi}{4}$	$ \bar{\nu}_{l_k} $
2	5.82	4.68	4.52	6.35	5.68	6.66	7.65	2	5.36
3	8	8	8	8	8	8	8	8	8
4	9.84	4.23	3.62	7.66	4.49	2.38	6.30	2	4.38
5	0	0	0	0	0	0	0	0	0

(b) $c'_{l_k} = 2$									
l'_k	$\theta=0$	$\theta=\frac{\pi}{4}$	$\theta=\frac{\pi}{2}$	$\theta=\frac{3\pi}{4}$	$\theta=\pi$	$\theta=\frac{5\pi}{4}$	$\theta=\frac{3\pi}{2}$	$\theta=\frac{7\pi}{4}$	$ \bar{\nu}_{l_k} $
2	7.66	6.66	5.68	6.36	4.53	4.68	5.82	2	4.15
3	0	0	0	0	0	0	0	0	0
4	4.22	3.62	7.66	4.48	2.38	6.30	2	9.84	5.18
5	11.31	11.31	11.31	11.31	11.31	11.31	11.31	11.31	11.31

Analogous to T_1 , T_2 is approximated by the Gaussian distribution with mean μ_{T_2} and variance $\sigma_{T_2}^2$. Under the hypothesis \mathcal{H}_0 , i.e., $\mathbf{b}_{l_k, \theta_q}$ has not been selected,

$$\begin{aligned} \mu_{T_2} | \mathcal{H}_0 &= MP |\nu_{l_k}|^2 / N_2 + M\sigma^2 \\ \sigma_{T_2}^2 | \mathcal{H}_0 &= 2MP |\nu_{l_k}|^2 / N_2 + M\sigma^2. \end{aligned} \quad (28)$$

Under the hypothesis \mathcal{H}_1 , i.e., $\mathbf{b}_{l_k, \theta}$ has been selected,

$$\begin{aligned} \mu_{T_2} | \mathcal{H}_1 &= MP N_2 + MP |\nu_{l_k}|^2 / N_2 + M\sigma^2 \\ \sigma_{T_2}^2 | \mathcal{H}_1 &= 2MP N_2 + 2MP |\nu_{l_k}|^2 / N_2 + M\sigma^2. \end{aligned} \quad (29)$$

Similarly, the decision threshold λ_2 satisfies the condition that

$$f_{T_2 | \mathcal{H}_0}(\lambda_2) = f_{T_2 | \mathcal{H}_1}(\lambda_2). \quad (30)$$

The probability of non-orthogonal sequence detection is

$$\begin{aligned} P_{d_2} &= Pr(T_2 \geq \lambda_2 | \mathcal{H}_1) \\ &= Q\left(\frac{\lambda_2 - MP N_2 - MP |\nu_{l_k}|^2 / N_2 - M\sigma^2}{\sqrt{2MP N_2 + 2MP |\nu_{l_k}|^2 / N_2 + M\sigma^2}}\right). \end{aligned} \quad (31)$$

Since the phase rotations have been detected, the collided users can be identified and the channel vector can be estimated as

$$\hat{\mathbf{h}}_k = \frac{1}{N_2 \sqrt{P}} \mathbf{Y}_2 \mathbf{s}_{l_k}^H, \quad (32)$$

with

$$\mathbf{s}_{l_k} = [\mathbf{a}_{l_k}, \mathbf{b}_{l_k, \theta_k}]. \quad (33)$$

Note that for $l_k \in \mathcal{K}_n$, if only one θ_k has been detected, it declares that $l_k \in \mathcal{K}_o$, which indicates that there is a false alarm in the orthogonal sequence detection and it has been corrected in the non-orthogonal sequence detection. The whole detection process is summarized in Algorithm 1.

The complexity of orthogonal detection is $\mathcal{O}(MN_1^2)$. As for other steps, denote the size of \mathcal{K}_o and \mathcal{K}_n as K_o and K_n , where $K_o + K_n = K$. Then, the complexity of interference cancellation and non-orthogonal sequence detection are $\mathcal{O}(K_o MN_2 Q + MN)$ and $\mathcal{O}(K_n MN_2 Q)$, respectively. Therefore, the complexity of Algorithm 1 is $\mathcal{O}(MN_1^2 + KMN_2 Q + MN)$.

Algorithm 1 Detection Algorithm of The Preamble with Phase Rotation

Input: The received signal $\mathbf{Y} = [\mathbf{Y}_1, \mathbf{Y}_2]$, decision threshold $\lambda_1, \lambda_2, \mathcal{K}_o = \emptyset, \mathcal{K}_n = \emptyset$.

Output: $\mathcal{K}_o = \{l_k | \mathbf{a}_{l_k} \text{ has been selected by one user}\}$,
 $\Lambda = \{(l_k, \theta_k) | \mathbf{b}_{l_k, \theta_k} \text{ has been selected by the user colliding in choosing } \mathbf{a}_{l_k}\}$.

Orthogonal sequence detection

```

1: for  $l_k = 1 : L_1$  do
2:   Calculate  $T_1 = \frac{1}{N_1} \|\mathbf{Y}_1 \mathbf{a}_{l_k}^H\|^2$ .
3:   if  $T_1 > \lambda_1$  then
4:      $\mathbf{a}_{l_k}$  has been used by  $K_c = \max\left(1, \frac{T_1}{MN_1P}\right)$  users.
5:     if  $K_c = 1$  then
6:        $l_k \in \mathcal{K}_o$ .
7:     else
8:        $l_k \in \mathcal{K}_n$ .
9:     end if
10:  else
11:     $\mathbf{a}_{l_k}$  has not been used.
12:  end if
13: end for

```

Interference cancellation

```

14: while  $l_k \in \mathcal{K}_o$  do
15:   Find the phase rotation of  $\mathbf{b}_{l_k, \theta_k}$  according to (22).
16: end while
17: Estimate the channel vector and obtain the residual signal of  $\mathbf{Y}_2$  according to (18).

```

Non-orthogonal sequence detection

```

18: while  $l_k \in \mathcal{K}_n$  do
19:   for  $q = 1 : \text{length}(\Theta)$  do
20:      $\theta_q = \Theta(q), T_2 = \frac{1}{N_2} \|\mathbf{Y}_2 \mathbf{b}_{l_k, \theta_q}^H\|^2$ .
21:     if  $T_2 > \lambda_2$  then
22:        $\theta_q$  has been used,  $(l_k, \theta_q) \in \Lambda$ .
23:     else
24:        $\theta_q$  has not been used.
25:     end if
26:   end for
27:   if The length of detected  $\theta_q$  is 1 then
28:     Only one user has selected  $\mathbf{a}_{l_k}$ , remove  $(l_k, \theta_q)$  from  $\Lambda, l_k \in \mathcal{K}_o$ .
29:   end if
30: end while

```

C. Performance analysis

With the proposed preambles, the probability that there is no preamble collision between k_{th} user and other $K - 1$ users is

$$P_{\text{nc}} = \left(1 - \frac{1}{QN_1}\right)^{K-1}. \quad (34)$$

The probability that there is no orthogonal preamble collision between k_{th} user and other $K - 1$ users is

$$P_{\text{noc}} = \left(1 - \frac{1}{N_1}\right)^{K-1}. \quad (35)$$

For the k_{th} active user, the probability of detection is

$$P_{d_k} = P_{\text{noc}}P_{d_1} + (P_{\text{nc}} - P_{\text{noc}})P_{d_c}P_{d_2}, \quad (36)$$

where P_{d_c} is the probability that $K_c > 1$, that is, $T_1 \geq \lambda_1$ and $T_1 \geq MN_1P$. In other words, $T_1 \geq \lambda_{\text{max}}$, where $\lambda_{\text{max}} = \max(\lambda_1, MN_1P)$. When user k collides with $K_c - 1$ users, the mean and variance of T_1 are

$$\begin{aligned} \mu_{T_1} | K_c &= K_c MN_1P + M\sigma^2, \\ \sigma_{T_1}^2 | K_c &= K_c(K_c - 1)MN_1^2P + M\sigma^2. \end{aligned} \quad (37)$$

Therefore, the probability that $K_c > 1$ is

$$P_{d_c} = Q\left(\frac{\lambda_{\text{max}} - K_c MN_1P - M\sigma^2}{\sqrt{K_c(K_c - 1)MN_1^2P + M\sigma^2}}\right). \quad (38)$$

The channel estimation error mainly results from the non-orthogonal sequences. In detail,

$$\begin{aligned} \hat{\mathbf{h}}_k^n &= \frac{1}{N_2\sqrt{P}}\mathbf{Y}_2\mathbf{b}_{l_k, \theta_k}^H \\ &= \mathbf{h}_k^n + \sum_{i=1}^{K_c^1} \frac{\nu_{\theta_k}}{N_2} + \sum_{j=1}^{K_c^2} \frac{\nu_{l_k}}{N_2} + \frac{\tilde{\mathbf{w}}}{N_2\sqrt{P}} \\ &= \mathbf{h}_k^n + \frac{K_c^1 \bar{\nu}_{\theta_k}}{N_2} + \frac{K_c^2 \bar{\nu}_{l_k}}{N_2} + \frac{\tilde{\mathbf{w}}}{N_2\sqrt{P}}, \end{aligned} \quad (39)$$

where K_c^1 is the number of users that select preambles with the same l_k , K_c^2 is the number of users that also suffer from preamble collisions despite choosing other orthogonal preambles. $\bar{\nu}_{\theta_k}$ and $\bar{\nu}_{l_k}$ are the mean of ν_{θ_k} and ν_{l_k} , respectively. $\tilde{\mathbf{w}} = \mathbf{W}\mathbf{b}_{l_k, \theta_k}^H \sim \mathcal{CN}(0, \mathbf{I}_M)$.

The channel estimation error is calculated as

$$\begin{aligned} e_{\mathbf{h}} &= \hat{\mathbf{h}}_k^n - \mathbf{h}_k^n \\ &= \frac{K_c^1 \bar{\nu}_{\theta_k}}{N_2} + \frac{K_c^2 \bar{\nu}_{l_k}}{N_2} + \frac{\tilde{\mathbf{w}}}{N_2\sqrt{P}}. \end{aligned} \quad (40)$$

As mentioned in Section III-B, $|\bar{\nu}_{l_k}|$ is generally reduced by the differential phase rotations. In other words, the CE errors caused by non-orthogonal sequences depending on $\bar{\nu}_{\theta_k}$ and $\bar{\nu}_{l_k}$ are reduced.

IV. EXTENSION OF THE PROPOSED PREAMBLE

The above analysis assumes adding phase rotation to the multiple root ZC sequences with a zero cyclic offset, but the scheme can be also extended to multiple root ZC sequences with different cyclic shifts. Then the non-orthogonal preamble is given as

$$b_{l_k, c_k, \theta_k}(n) = \exp\left(\frac{-j\pi l_k(n + c_k)(n + c_k + 1)}{N_2} - jn\theta_k\right), \quad (41)$$

where c_k is the cyclic shift randomly selected in the range of $[1, C_{\text{max}}]$, and θ_k is randomly selected from the set Θ .

It is obvious that the cross-correlation $|\mathbf{b}_{l_k, c_k, \theta_k} \mathbf{b}_{l_k, c_q, \theta_q}^H|$ is related to $l_k, c_q - c_k$ and $\theta_q - \theta_k$. To avoid the worst situation that $|\mathbf{b}_{l_k, c_k, \theta_k} \mathbf{b}_{l_k, c_q, \theta_q}^H| = N_2$, with given l_k , the selection of the cyclic shift and phase rotation should satisfy Lemma 1.

Lemma 1: For any $\theta_q, \theta_k \in \Theta$ and any $c_q, c_k \in [1, C_{\max}]$, the following condition should to be met.

$$\frac{2l_k\pi(c_q - c_k)}{N_2} + \theta_q - \theta_k \neq 2\alpha\pi, \alpha = 0, 1, 2, \dots \quad (42)$$

Proof: Due to the properties of ZC sequences, sequences with different roots can be detected by comparing the correlation with a threshold. But for sequences with the same root but different c_k or θ_k , the cross-correlation is calculated as

$$G = \left| \mathbf{b}_{l_k, c_k, \theta_k} \mathbf{b}_{l_k, c_q, \theta_q}^H \right| = \left| \sum_{n=1}^{N_2} \exp \left(jn \left(\frac{2l_k\pi\Delta_c}{N_2} + \Delta_\theta \right) + \frac{jl_k\pi D}{N_2} \right) \right|. \quad (43)$$

Here, $\Delta_c = c_q - c_k$, $\Delta_\theta = \theta_q - \theta_k$ and $D = \Delta_c(c_q + c_k + 1)$. G is much less than N_2 in the case of $c_q = c_k, \theta_q \neq \theta_k$ and $c_q \neq c_k, \theta_q = \theta_k$. However, when $\frac{2l_k\pi\Delta_c}{N_2} + \Delta_\theta = 0, 2\pi, 4\pi, \dots$, $G = N_2$ even if $c_q \neq c_k, \theta_q \neq \theta_k$, which leads to false detections. Therefore, to avoid this situation, Δ_c and Δ_θ are supposed to satisfy that

$$\frac{2l_k\pi\Delta_c}{N_2} + \Delta_\theta \neq 2\alpha\pi, \alpha = 0, 1, 2, \dots \quad (44)$$

For example, assuming that $\Theta = [0, \pi/2, \pi, 3\pi/2]$ and $l_k = 1$, (42) is

$$\Delta_c \neq \alpha N_2 - \frac{\Delta_\theta N_2}{2\pi}, \alpha = 0, 1, 2, \dots \quad (45)$$

Since $\Delta_c < N_2$ and $\Delta_\theta < 2\pi$, (45) always holds when $\alpha > 1$. Then the problem is to find C_{\max} so that $\Delta_c \neq -\frac{\Delta_\theta N_2}{2\pi}$ and $\Delta_c \neq N_2 - \frac{\Delta_\theta N_2}{2\pi}$. With the given Θ ,

$$\left| -\frac{\Delta_\theta N_2}{2\pi} \right| = \left\{ \frac{N_2}{4}, \frac{N_2}{2}, \frac{3N_2}{4} \right\}, \left| N_2 - \frac{\Delta_\theta N_2}{2\pi} \right| = \left\{ \frac{N_2}{4}, \frac{N_2}{2}, \frac{3N_2}{4}, \frac{5N_2}{4}, \frac{3N_2}{2}, \frac{7N_2}{4} \right\}. \quad (46)$$

Therefore, it is derived that $\Delta_c < \frac{N_2}{4}$ and thus $C_{\max} = \lfloor \frac{N_2}{4} + 1 \rfloor$.

Similarly, the setting of Θ and C_{\max} for other values of l_k can be derived.

V. SIMULATION RESULTS

In this section, simulations are performed to evaluate the performance of the designed preamble. Simulation results in terms of the probability of AUD, normalized mean square error (NMSE) of CE and success rate defined in [26] are presented to verify the effectiveness of the proposed composite preamble. The orthogonal preambles, auxiliary preambles assisted by multiple root ZC sequences without phase rotations [15] and aggregate preambles based on orthogonal sequences [22] are chosen as comparisons.

A. Performance of AUD

The probability of no preamble collision is given in Fig. 4, where N is fixed as 64. It is shown that the probability of no preamble collisions P_{nc} is much increased with differential rotations, especially when the number of active users is larger than the preamble length, that is $K > 60$. In particular, the more phase rotations available and the longer the orthogonal sequence, i.e., the larger the Q and N_1 , the larger P_{nc} . However, although collisions can be reduced by increasing the length of orthogonal sequences, the performance of AUD cannot be consistently improved as N_1 increases.

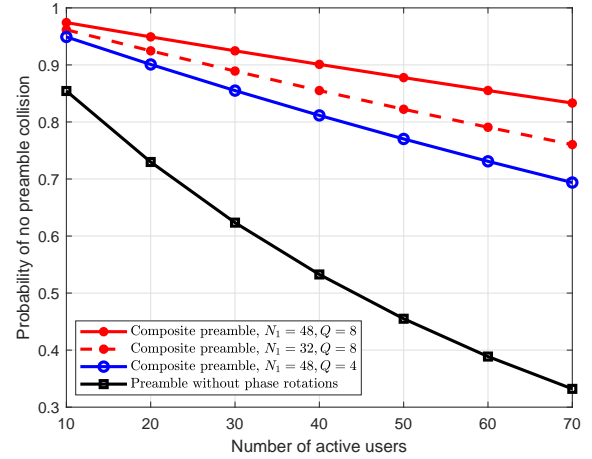


Fig. 4. Probability of no preamble collision.

The variation of detection performance with N_1 is shown in Fig. 5, where the numerical results are consistent with the theoretical ones. The length of the preamble is $N = 64$, and phase rotations are randomly selected from $\Theta = [\pi/4, \pi/2, 3\pi/4, \pi, 5\pi/4, 3\pi/2, 7\pi/4, 2\pi]$. It is obvious that there is an optimal N_1 that maximizes P_d , and the optimal N_1 is closely related to communication conditions. First, the performance is improved with increasing N_1 , because the longer orthogonal sequence enlarges the preamble set size and contributes to accurate detection. However, the length of non-orthogonal sequences N_2 is decreased with N_1 , which limits non-orthogonal sequence detection accuracy. In addition, as N_1 increases, N_1 has a diminishing effect on reducing the probability of orthogonal preamble collisions, and the performance of AUD mainly depends on non-orthogonal sequences. Therefore, the performance first increases with N_1 , but when N_1 has little effect on reducing orthogonal preamble collisions and it reduces the non-orthogonal sequence detection performance significantly, the detection accuracy decreases as the orthogonal sequences become longer.

The simulation results under conditions with different N_2 and Θ is given as Fig. 6, where $M = 10$ and $\text{SNR} = -5$ dB. $\Delta_\theta = \frac{\pi}{3}$ means $\Theta = [\pi/3, 2\pi/3, \pi, 4\pi/3, 5\pi/3, 2\pi]$ and $\Delta_\theta = \frac{\pi}{4}$ means $\Theta = [\pi/4, \pi/2, 3\pi/4, \pi, 5\pi/4, 3\pi/2, 7\pi/4, 2\pi]$. It is obvious that there is always an optimal N_2 that maximizes the detection performance, which can be explained by the fact that increasing N_2 enlarges the size of the preamble pool and increases the performance of the non-orthogonal detection

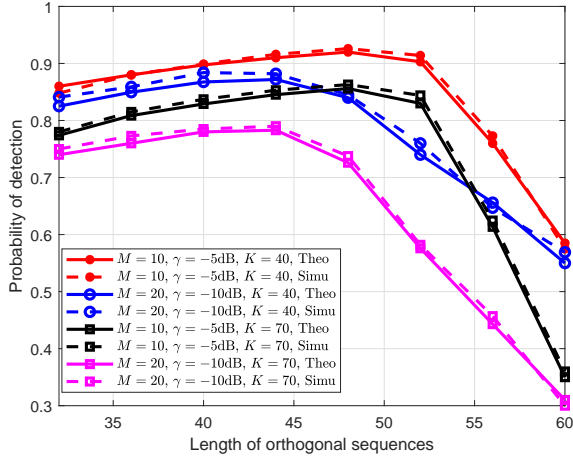


Fig. 5. Probability of detection with various N_1 .

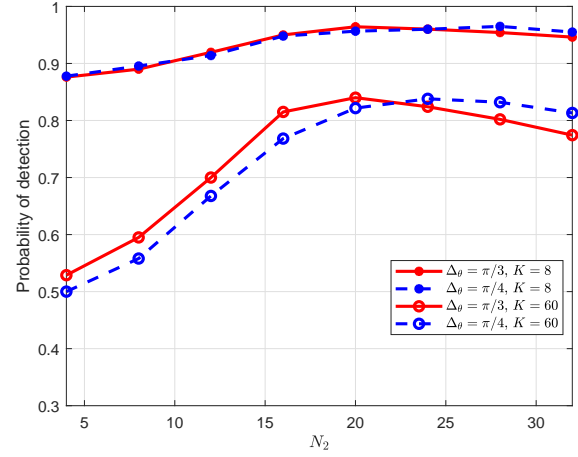


Fig. 6. Performance under conditions with different N_2 and Θ .

to some extent but also reduces the performance orthogonal sequences. As for Θ , it is used to enlarge the preamble pool at the cost of introducing more nonorthogonality, and the smaller Δ_θ , the larger of the preamble pool. The importance of orthogonal or non-orthogonal detection depends on the number of users. When K is small, orthogonal detection plays a dominant role, and smaller Δ_θ makes no difference since it is unnecessary to further expand the preamble pool. However, when K is as large as 60, orthogonal preamble collisions are inevitable and Θ is needed. It is worth noting that when $N_2 \leq 20$, larger Δ_θ performs better, while things are quite different when $N_2 > 20$. That is because in the case of $N_2 \leq 20$, i.e., $N_1 \geq 44$, the probability of preamble collision is low and users can be detected as long as users colliding in orthogonal preambles can be identified, which indicates that improving the detection performance of non-orthogonal detection is more important than expanding the preamble pool. Since the overall interference of $\Delta_\theta = \frac{\pi}{3}$ is smaller, it performs better. But when $N_2 > 20$, the probability of preamble collision is high, and solving the collision problem is more critical. Therefore, $\Delta_\theta = \frac{\pi}{4}$ outperforms $\Delta_\theta = \frac{\pi}{3}$ even though its interference is larger.

which cannot be mitigated in secondary preambles without phase rotations.

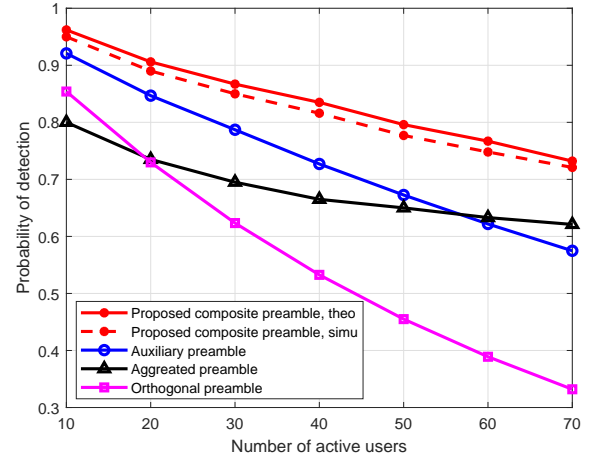


Fig. 7. Probability of detection.

Fig. 7 compares the performance of AUD of the proposed preamble with other schemes, where $M = 10$, $\gamma = -5$ dB. The preamble length and phase rotations set are $N_1 = N_2 = 32$ and $\Theta = [\pi/4, \pi/2, 3\pi/4, \pi, 5\pi/4, 3\pi/2, 7\pi/4, 2\pi]$. Without avoiding preamble collisions, the performance of preambles used in LTE decrease dramatically due to the high probability of collisions, which is not the case with other schemes that consider preamble collisions. As for preambles considering collisions avoidance, the proposed preamble performs better than the other two, where the numerical results accord with the theoretical ones. In particular, the performance advantage of composite preambles over auxiliary preambles becomes more significant as the number of active users increases. That is because the number of collided users increases with K , and so does the non-orthogonal interference. In such cases, with the help of differential phase rotations, the non-orthogonality is reduced in the designed preamble,

B. Performance of CE and success rate

The performance of CE is measured by the average NMSE, which is calculated as

$$\text{NMSE} = \frac{1}{I} \sum_{i=1}^I \frac{\|\hat{\mathbf{h}}_{k,i} - \mathbf{h}_{k,i}\|^2}{\|\mathbf{h}_{k,i}\|^2}, \quad (47)$$

where $\hat{\mathbf{h}}_{k,i}$ and $\mathbf{h}_{k,i}$ are the estimated and exact channel vectors of user k in i_{th} Monte Carlo simulation, respectively. I is the number of Monte Carlo simulations. The simulation results under different SNR conditions are presented in Fig. 8, where $M = 40$, $K = 50$, and $N_1 = 40$, $N = 64$. Θ is the same as Fig. 7. It's shown that the estimation errors of the proposed preamble is less than other preambles. It is worth noting that the NNSE curves of the proposed preamble and aggregated preamble are getting closer and closer when $\text{SNR} > 0$ dB, and they almost intersect at $\text{SNR} = 6$ dB.

Since two orthogonal preambles with different power levels are adopted in the aggregated preamble, the detection performance of preambles under low SNR conditions cannot be guaranteed due to the inaccurate detection of power levels, which leads to the larger deviation of CE. However, as the SNR increases, the detection probability of aggregated preambles gradually approaches 1. In addition, as a consequence of random combinations of orthogonal sequences and power levels, its preamble set size is greatly enlarged and the probability of preamble collisions is the lowest among the four mentioned schemes. Therefore, the CE error of aggregated preambles is pretty low under high SNR conditions. As for the proposed composite preambles, even though the probability of no collisions is lower than aggregated preambles, it is still close to 0.9, which is sufficient for a low estimation error with the assistance of higher detection probability. Hence, the NMSE of proposed composite preamble is much lower than benchmarks under low SNR conditions, and it gradually approaches the extremely low level that is close to the NMSE of aggregated preambles under high SNR conditions.

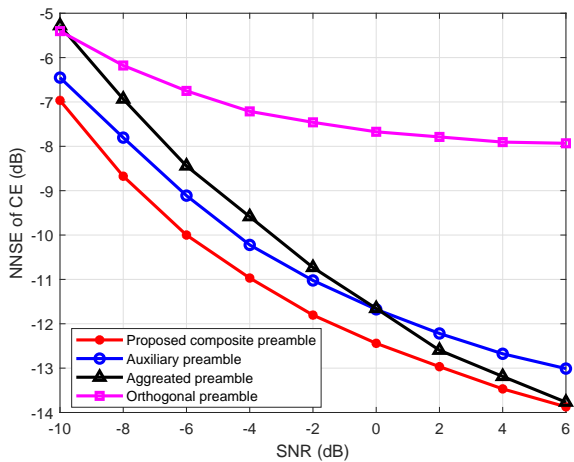


Fig. 8. NMSE of CE under various SNR conditions.

The NMSE of CE vs. the number of active users is plotted in Fig. 9, where SNR = -5 dB and other simulation parameters are set to be the same as Fig. 8. It is obvious that the more active users, the larger NMSE, which is caused by the increased probability of preamble collision. In addition, in terms of the increasing rate of NMSE with respect to K , the proposed preamble outperforms the auxiliary and orthogonal preambles due to the more enlarged preamble set size. Furthermore, compared with the aggregated preambles, the proposed preamble is slightly worse in increasing rate since its rate is larger, but it performs better owing to the higher detection probability.

The success rate of the proposed preamble and comparisons under conditions with different SINR thresholds are shown in Fig. 10, where SNR = 0 dB and other parameters are set to be the same as the above simulations. The success rate is defined in [26] to evaluate the success access probability, which is mainly related to the probability of preamble collision and CE performance. Specifically, the success rate of k_{th} user is

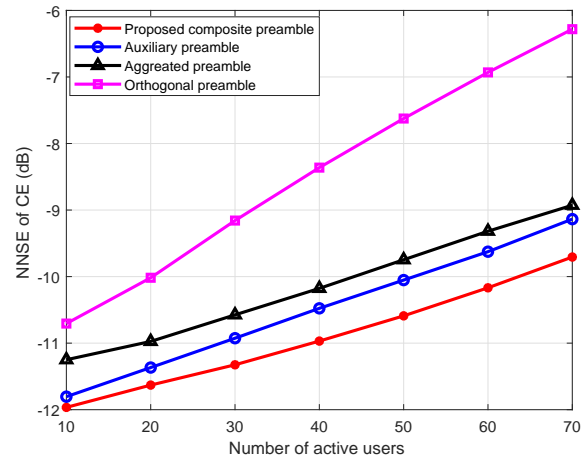


Fig. 9. NMSE of CE with different number of active users.

calculated as

$$P_{\text{suc}} = P_{\text{nc}} P(\gamma_k^I > \gamma_{\text{th}}^I), \quad (48)$$

where γ_k^I is the received signal to interference and noise ratio (SINR), which is calculated based on the recovered signal

$$\mathbf{y}_k = \hat{\mathbf{h}}_k^H \mathbf{Y}. \quad (49)$$

γ_{th}^I is the SINR threshold. Similarly, since the proposed composite preamble reduces preamble collision with low non-orthogonality, it is superior to other preambles in terms of success rate.

C. Performance of the proposed preamble with multiple cyclic shifts

The performance of the composite preambles with multiple cyclic shifts and phase rotations in terms of the probability of detection and success rate are given in Fig. 11 and Fig. 12, respectively. Here, $M = 40$, SNR = 0 dB and the preamble length is $N = 64$ with $N_1 = 32$. Phase rotations are randomly selected from $\Theta_1 = [0, \pi/4, \pi/2, 3\pi/4, \pi, 5\pi/4, 3\pi/2, 7\pi/4]$ or $\Theta_2 = [0, \pi/2, \pi, 3\pi/2]$, and the cyclic shifts are obtained based on Lemma 1 accordingly. It's shown that the combination of cyclic shifts and phase rotations improves the probability of detection and success rate. Note that the performance improvement is more significant in the case of Θ_2 , which can be explained by the fact that C_{max} is related to Δ , and the larger the Δ_θ , the more cyclic shifts are available.

VI. CONCLUSION

In this paper, a composite preamble consisting of orthogonal sequences and non-orthogonal sequences with differential phase rotations is designed to reduce the non-orthogonal interference while reducing the probability of preamble collisions, and thereby improving the performance of AUD and CE. Accordingly, the detection algorithm and CE scheme are also proposed, and the performance is analyzed theoretically. It is shown that differential phase rotations enables the expansion

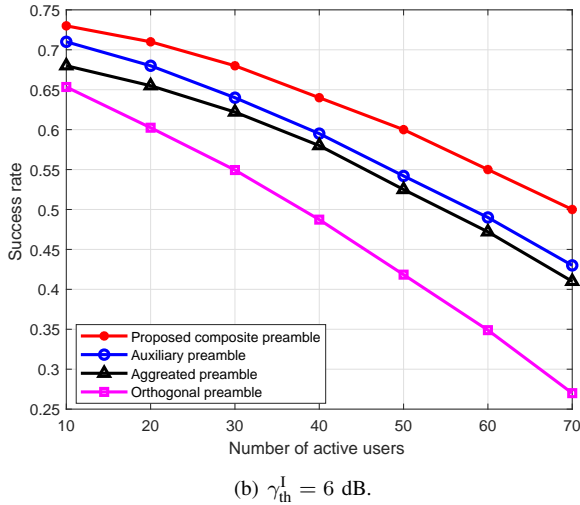
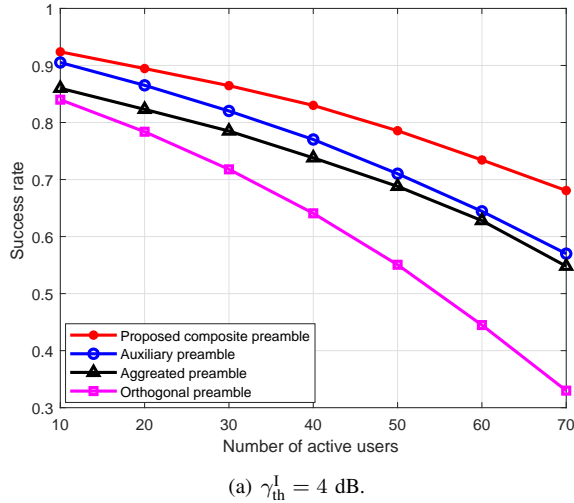


Fig. 10. Success rate of the proposed preamble and benchmarks.

of preamble set size and the reduction of non-orthogonality. Simulation results shows that the designed preamble performs better than orthogonal sequence-based preambles and non-orthogonal preambles without phase rotations.

For the design and extension of the composite preamble, there are some other issues to be studied. For example, as shown in Fig. 5 and Fig. 6, there always exists an optimal length of orthogonal sequences that maximizes the detection performance under different conditions, and the optimal length has an influence on the design of the phase set. Therefore, further research is needed to adaptively determine the optimal length of orthogonal sequences and phase sets according to the conditions. In addition, The preamble is proposed for the single-cell system, whose performance degrades in the multi-cell scenario. To extend the proposed scheme to multi-cell scenarios, the design of the composite preamble needs to be improved to reduce the inter-cell interference, and introducing cell-specific power coefficients in the proposed preamble is a promising way. Moreover, GFRA has great potential in other scenarios, including ultra-reliable low-latency communication-

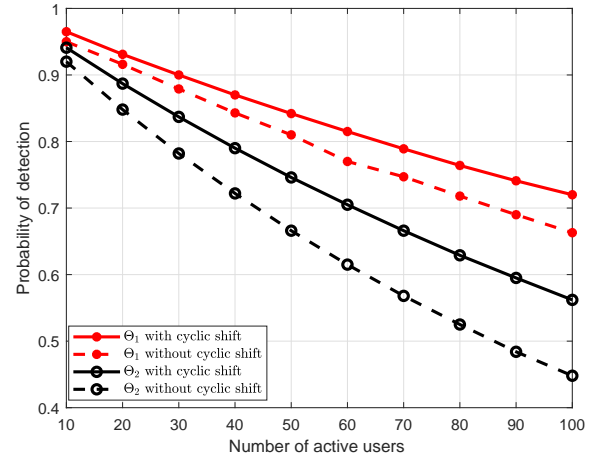


Fig. 11. Comparison of detection performance between preambles with and without cyclic shifts.

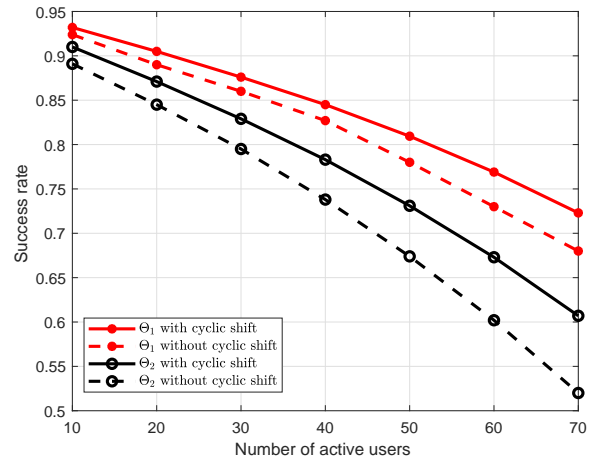


Fig. 12. Comparison of success rate between preambles with and without cyclic shifts in the case of $\gamma_{th}^I = 4$ dB.

s (URLLC), cell-free MIMO, and unmanned aerial vehicle (UAV) networks, etc.. How to solve the preamble transmission and detection in these scenarios is still an open issue.

REFERENCES

- [1] M. B. Shahab, R. Abbas, M. Shirvanimoghaddam, and S. J. Johnson, "Grant-free non-orthogonal multiple access for IoT: A survey," *IEEE Commun. Surveys Tuts.*, vol. 22, no. 3, pp. 1805–1838, 2020.
- [2] Cisco, "Cisco annual internet report (20182023)," White Paper, Mar. 2020.
- [3] Ericsson, "Ericsson mobility report," Ericsson, Stockholm, Sweden, Technical Report EAB-18:004510Uen, Revision A, Jun. 2018.
- [4] ITU-R, "IMT vision-framework and overall objectives of the future development of IMT for 2020 and beyond," Int. Telecommun. Union, Geneva, Switzerland, ITU Recommendation M.2083-0, Sep. 2015.
- [5] Y. Cui, W. Xu, Y. Wang, J. Lin, and L. Lu, "Side-information aided compressed multi-user detection for up-link grant-free NOMA," *IEEE Trans. Wireless Commun.*, vol. 19, no. 11, pp. 7720–7731, 2020.
- [6] S. Kim, J. Kim, and D. Hong, "A new non-orthogonal transceiver for asynchronous grant-free transmission systems," *IEEE Trans. Wireless Commun.*, vol. 20, no. 3, pp. 1889–1902, 2021.
- [7] L. Liu and W. Yu, "Massive connectivity with massive MIMO-Part 1: Device activity detection and channel estimation," *IEEE Trans. Signal Process.*, vol. 66, no. 11, pp. 2933–2946, 2018.

- [8] J. Ahn, B. Shim, and K. B. Lee, "EP-based joint active user detection and channel estimation for massive machine-type communications," *IEEE Trans. Commun.*, vol. 67, no. 7, pp. 5178–5189, 2019.
- [9] S. Jiang, X. Yuan, X. Wang, C. Xu, and W. Yu, "Joint user identification, channel estimation, and signal detection for grant-free NOMA," *IEEE Trans. Wireless Commun.*, vol. 19, no. 10, pp. 6960–6976, 2020.
- [10] J. Zhang, Y. Pan, and J. Xu, "Compressive sensing for joint user activity and data detection in grant-free NOMA," *IEEE Wireless Commun. Lett.*, vol. 8, no. 3, pp. 857–860, 2019.
- [11] X. Miao, D. Guo, and X. Li, "Grant-free NOMA with device activity learning using Long Short-Term Memory," *IEEE Wireless Commun. Lett.*, vol. 9, no. 7, pp. 981–984, 2020.
- [12] J. Ding, D. Qu, H. Jiang, and T. Jiang, "Success probability of grant-free random access with massive MIMO," *IEEE Internet of Things Journal*, vol. 6, no. 1, pp. 506–516, 2019.
- [13] Y. Liang, X. Li, J. Zhang, and Z. Ding, "Non-orthogonal random access for 5G networks," *IEEE Trans. Wireless Commun.*, vol. 16, no. 7, pp. 4817–4831, 2017.
- [14] E. de Carvalho, E. Björnson, J. H. Sørensen, E. G. Larsson, and P. Popovski, "Random pilot and data access in massive mimo for machine-type communications," *IEEE Trans. Wireless Commun.*, vol. 16, no. 12, pp. 7703–7717, 2017.
- [15] S. Kim, H. Kim, H. Noh, Y. Kim, and D. Hong, "Novel transceiver architecture for an asynchronous grant-free IDMA system," *IEEE Trans. Wireless Commun.*, vol. 18, no. 9, pp. 4491–4504, 2019.
- [16] H. Jiang, D. Qu, J. Ding, and T. Jiang, "Multiple preambles for high success rate of grant-free random access with massive MIMO," *IEEE Trans. Wireless Commun.*, vol. 18, no. 10, pp. 4779–4789, 2019.
- [17] J. Choi, "An approach to preamble collision reduction in grant-free random access with massive MIMO," *IEEE Trans. Wireless Commun.*, vol. 20, no. 3, pp. 1557–1566, 2021.
- [18] J. Ding and J. Choi, "Comparison of preamble structures for grant-free random access in massive MIMO systems," *IEEE Wireless Commun. Lett.*, vol. 9, no. 2, pp. 166–170, 2020.
- [19] A. Quayum, Y. Kakishima, H. Minn, and H. Papadopoulos, "Non-orthogonal pilot designs with collision detection capability for grant-free access," in *2018 IEEE International Conference on Communications (ICC)*, 2018, pp. 1–6.
- [20] A. Quayum, H. Minn, and Y. Kakishima, "Non-orthogonal pilot designs for joint channel estimation and collision detection in grant-free access systems," *IEEE Access*, vol. 6, pp. 55 186–55 201, 2018.
- [21] G. S. Harini, N. Mysore Balasubramanya, and M. Rana, "On preamble-based grant-free transmission in low power wide area (LPWA) IoT networks," in *2020 IEEE 6th World Forum on Internet of Things (WF-IoT)*, 2020, pp. 1–6.
- [22] A. E. Mostafa, V. W. S. Wong, S. Liao, R. Schober, M. Ding, and F. Wang, "Aggregate preamble sequence design for massive machine-type communications in 5G networks," in *2018 IEEE Global Communications Conference (GLOBECOM)*, 2018, pp. 1–6.
- [23] A. E. Mostafa, V. W. Wong, Y. Zhou, R. Schober, Z. Luo, S. Liao, and M. Ding, "Aggregate preamble sequence design and detection for massive IoT with deep learning," *IEEE Trans. Veh. Technol.*, vol. 70, no. 4, pp. 3800–3816, 2021.
- [24] K. Senel and E. G. Larsson, "Grant-free massive MTC-enabled massive MIMO: A compressive sensing approach," *IEEE Trans. Commun.*, vol. 66, no. 12, pp. 6164–6175, 2018.
- [25] R.-A. Pitaval, B. M. Popovic, F. Berggren, and P. Wang, "Overcoming 5G PRACH capacity shortfall by combining Zadoff-Chu and m-sequences," in *2018 IEEE International Conference on Communications (ICC)*, 2018, pp. 1–6.
- [26] J. Ding, D. Qu, and J. Choi, "Analysis of non-orthogonal sequences for grant-free ra with massive MIMO," *IEEE Trans. Commun.*, vol. 68, no. 1, pp. 150–160, 2020.
- [27] L. Bai, J. Liu, Q. Yu, J. Choi, and W. Zhang, "A collision resolution protocol for random access in massive MIMO," *IEEE J. Sel. Areas Commun.*, vol. 39, no. 3, pp. 686–699, 2021.
- [28] R. Tandra and A. Sahai, "SNR walls for signal detection," *IEEE J. Sel. Topics Signal Process.*, vol. 2, no. 1, pp. 4–17, 2008.
- [29] Y.-C. Liang, Y. Zeng, E. C. Peh, and A. T. Hoang, "Sensing-throughput tradeoff for cognitive radio networks," *IEEE Trans. Wireless Commun.*, vol. 7, no. 4, pp. 1326–1337, 2008.
- [30] J. Font-Segura, G. Vazquez, and J. Riba, "Sampling walls in signal detection of bernoulli nonuniformly sampled signals," in *2013 IEEE International Conference on Communications (ICC)*, 2013, pp. 4536–4540.



Yang Wang (Student Member, IEEE) is a Ph.D. student in School of Artificial Intelligence, Beijing University of Posts and Telecommunications, Beijing, China. She received the B.S. degree from the School of Information and Communication Engineering, Beijing University of Posts and Telecommunications, Beijing, China, in 2018. Her current research interests include wireless sensing and statistical signal processing.



Wenjun Xu (Senior Member, IEEE) is a professor with the State Key Laboratory of Network and Switching Technology, Beijing University of Posts and Telecommunications, Beijing, China, and with Peng Cheng Laboratory, Shenzhen, China. He received his Ph.D. degree from Beijing University of Posts and Telecommunications, Beijing, China, in 2008. His research interests include artificial intelligence-driven networks, semantic communications, unmanned aerial vehicle communications and networks, green communications and networking.

He is an editor of *China Communications* and a Senior Member of IEEE.



Markku Juntti (Fellow, IEEE) was with University of Oulu in 1992C98. In academic year 1994C95, he was a Visiting Scholar at Rice University, Houston, Texas. In 1999C2000, he was a Senior Specialist with Nokia Networks in Oulu, Finland. Dr. Juntti has been a professor of communications engineering since 2000 at University of Oulu, Centre for Wireless Communications (CWC), where he leads the Communications Signal Processing (CSP) Research Group. He also serves as Head of CWC C Radio Technologies (RT) Research Unit. His research interests include signal processing for wireless networks as well as communication and information theory. He is an author or co-author in almost 500 papers published in international journals and conference records as well as in books *Wideband CDMA for UMTS in 2000C2010*, *Handbook of Signal Processing Systems in 2013 and 2018* and *5G Wireless Technologies in 2017*.

Dr. Juntti is also an Adjunct Professor at Department of Electrical and Computer Engineering, Rice University, Houston, Texas, USA. Dr. Juntti is an Editor of *IEEE Transactions on Wireless Communications*, and served previously in similar role in *IEEE Transactions on Communications* and *IEEE Transactions on Vehicular Technology*. He was Secretary of IEEE Communication Society Finland Chapter in 1996C97 and the Chair for years 2000C01. He has been Secretary of the Technical Program Committee (TPC) of the 2001 IEEE International Conference on Communications (ICC), and the Chair or Co-Chair of the Technical Program Committee of several conferences including 2006 and 2021 IEEE International Symposium on Personal, Indoor and Mobile Radio Communications (PIMRC), the Signal Processing for Communications Symposium of IEEE Globecom 2014, Symposium on Transceivers and Signal Processing for 5G Wireless and mm-Wave Systems of IEEE GlobalSIP 2016, ACM NanoCom 2018, and 2019 International Symposium on Wireless Communication Systems (ISWCS). He has also served as the General Chair of 2011 IEEE Communication Theory Workshop (CTW 2011) and 2022 IEEE Workshop on Signal Processing Advances in Wireless Communications (SPAWC).



Jiaru Lin (Member, IEEE) received the B.S. and Ph.D. degrees from the School of Information Engineering, Beijing University of Posts and Telecommunications (BUPT), China, in 1987 and 2001, respectively.

From 1991 to 1994, he studied at the Swiss Federal Institute of Technology, Zürich. He is currently a Professor and the Ph.D. Supervisor with the School of Artificial Intelligence, BUPT. His research interests include wireless communications, personal communication, and communication networks.



Miao Pan (S07-M12-SM18) received his BSc degree in Electrical Engineering from Dalian University of Technology, China, in 2004, MAsc degree in electrical and computer engineering from Beijing University of Posts and Telecommunications, China, in 2007 and Ph.D. degree in Electrical and Computer Engineering from the University of Florida in 2012, respectively. He is now an Associate Professor in the Department of Electrical and Computer Engineering at University of Houston. He was a recipient of NSF CAREER Award in 2014. His research interests

include Wireless/AI for AI/Wireless, deep learning privacy, cybersecurity, and underwater communications and networking. His work won IEEE TCGCC (Technical Committee on Green Communications and Computing) Best Conference Paper Awards 2019, and Best Paper Awards in ICC 2019, VTC 2018, Globecom 2017 and Globecom 2015, respectively.

Dr. Pan is an Editor for IEEE Open Journal of Vehicular Technology, an Associate Editor for ACM Computing Surveys and an Associate Editor for IEEE Internet of Things (IoT) Journal (Area 5: Artificial Intelligence for IoT), and used to be an Associate Editor for IEEE Internet of Things (IoT) Journal (Area 4: Services, Applications, and Other Topics for IoT) from 2015 to 2018. He has also been serving as a Technical Organizing Committee for several conferences such as TPC Co-Chair for Ubiquitous 2019, ACM WUWNet 2019. He is a member of AAAI, a member of ACM, and a senior member of IEEE.